Available online at www.sciencedirect.com
ScienceDirect
Phytochemistry 68 (2007) 1651–1663
PHYTOCHEMISTRY
www.elsevier.com/locate/phytochem

# Three oxidative metabolites of indole-3-acetic acid from *Arabidopsis thaliana*

Kenji Kai [a,c], Junko Horita [a], Kyo Wakasa [b,c], Hisashi Miyagawa [a,c,*]

[a] *Division of Applied Life Science, Graduate School of Agriculture, Kitashirakawa, Sakyo-ku, Kyoto University, Kyoto 606-8502, Japan*
[b] *Department of Agriculture, Tokyo University of Agriculture, Kanagawa 243-0034, Japan*
[c] *CREST, JST, Tokyo 103-0027, Japan*

Received 2 November 2006; received in revised form 16 April 2007
Available online 4 June 2007

**Abstract**

Three metabolites of indole-3-acetic acid (IAA), *N*-(6-hydroxyindol-3-ylacetyl)-phenylalanine (6-OH-IAA-Phe), *N*-(6-hydroxyindol-3-ylacetyl)-valine (6-OH-IAA-Val), and 1-*O*-(2-oxoindol-3-ylacetyl)-β-D-glucopyranose (OxIAA-Glc), were found by a liquid chromatography-electrospray ionization-tandem mass spectrometry (LC-ESI-MS/MS)-based search for oxidative IAA metabolites during the vegetative growth of *Arabidopsis*. Their structures were confirmed by making a comparison of chromatographic characteristics and mass spectra between naturally occurring compounds and synthetic standards. An incorporation study using deuterium-labeled compounds showed that 6-OH-IAA-Phe and 6-OH-IAA-Val were biosynthesized from IAA-Phe and IAA-Val, respectively, which strongly suggested the formation of these amino acid conjugates of IAA in plants. Both 6-OH-IAA-Phe and 6-OH-IAA-Val were inactive as auxins, as indicated by no significant root growth inhibition in *Arabidopsis*. Quantitative analysis demonstrated that OxIAA-Glc was present in the largest amount among the metabolites of IAA in *Arabidopsis*, suggesting that the conversion into OxIAA-Glc represents the main metabolic process regarding IAA in *Arabidopsis*.


*Keywords:* *Arabidopsis thaliana*; Cruciferae; Indole-3-acetic acid; IAA metabolites; Liquid chromatography-electrospray ionization-tandem mass spectrometry

## 1. Introduction

Indole-3-acetic acid (IAA, **1**) (Fig. 1) is one of the auxins that regulate plant growth and development as a plant hormone. Its levels are thought to be finely controlled by balancing the activities of its biosynthesis, metabolism, and transport to establish what is referred to as "IAA homeostasis". Considerable effort has also been directed at clarifying the processes and factors contributing to IAA homeostasis, but the entire picture remains to be elucidated (Normanly, 1997; Slovin et al., 1999; Normanly and Bartel, 1999; Ljung et al., 2002; Woodward and Bartel, 2005).

In plants, most IAA (**1**) is thought to be present in a conjugated form, since a large amount of IAA (**1**) is released by hydrolysis of plant extracts. Two distinct groups of bound IAA (**1**), or IAA conjugates, have been described in a variety of plant species. The first group includes the IAA esters. The conjugate with glucose is the one most studied: the enzymes involved both in its formation and in its hydrolysis have been characterized in several plants (Bandurski et al., 1995; Szerszen et al., 1994; Slovin et al., 1999; Jackson et al., 2001; Jackson et al., 2002). The second group is comprised of the amide compounds, in which IAA (**1**) is linked with various amino acids, such as Ala, Asp, Glu, and Leu (Östin et al., 1998; Barratt et al., 1999; Tam et al., 2000; Kowalczyk and Sandberg,

* Corresponding author. Address: Division of Applied Life Science, Graduate School of Agriculture, Kitashirakawa, Sakyo-ku, Kyoto University, Kyoto 606-8502, Japan. Tel./fax: +81 75 753 6123.
*E-mail address:* miyagawa@kais.kyoto-u.ac.jp (H. Miyagawa).

0031-9422/$ - see front matter © 2007 Elsevier Ltd. All rights reserved.
doi:10.1016/j.phytochem.2007.04.030

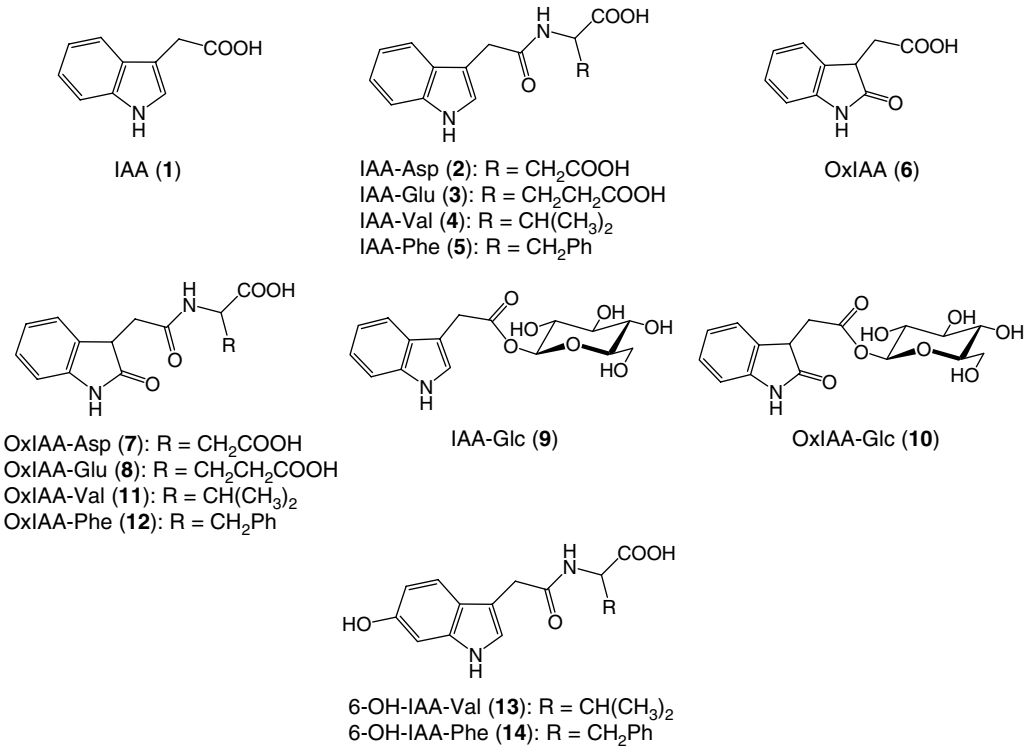


Fig. 1. Structures of IAA (**1**) and its metabolites.

2001). The presence of a peptide-bound IAA has also been demonstrated in the seeds of *Arabidopsis* and bean, and quite recently in strawberry fruit (Bialek and Cohen, 1986; Walz et al., 2002; Park et al., 2006).

Although a number of IAA conjugates have been identified to date, a considerable proportion of total bound IAA (**1**) is still chemically unknown in many plants (Normanly, 1997). In *Arabidopsis* in particular, IAA (**1**) and hitherto characterized IAA conjugates only account for a few persent of all the IAA (**1**) that is released after alkaline hydrolysis (Tam et al., 2000). To identify the unknown IAA conjugates, Kowalzcyk and Sandberg screened for IAA-amide compounds using GC–MS, finding IAA-Ala and IAA-Leu to be minor components (Kowalczyk and Sandberg, 2001). However, they failed to find any major compounds and concluded that no other conjugates were present in detectable amounts in *Arabidopsis* seedlings. Nonetheless, genetic analyses to date have shown that *Arabidopsis* has a variety of IAA amidohydrolases. For example, amide hydrolase ILR1 shows a high degree of highly specific for IAA-Leu and IAA-Phe (**5**) (Bartel and Fink, 1995; LeClere et al., 2002), although IAA-Phe (**5**) has never been found in plants until now. Furthermore, it was shown recently that the early-auxin inducible *GH3* genes encode IAA-amide synthase, and that these amide synthetases catalyze the formation of IAA-Asp (**2**), -Gln, -Glu (**3**), -Gly, -Ile, -Phe, -Tyr, and -Val (**4**) in vitro (Staswick et al., 2005). None of these conjugates, however, has been detected as an endogenous component in intact plants except for IAA-Asp (**2**) and IAA-Glu (**3**). These findings strongly suggest that many types of IAA-amide conjugates are present at levels below the detection limit and/or display a rapid turn over, playing a regulatory role *in planta*.

Besides the conjugation of IAA (**1**) with endogenous components, oxidation has been observed as a catabolic process in a variety of plants (Normanly, 1997). The best known oxidative metabolite is 2-oxoindole-3-acetic acid (OxIAA, **6**). The rapid formation of OxIAA (**6**) after plants were supplied with IAA (**1**) indicates the important role of OxIAA (**6**) in the homeostatic control of the hormone level (Östin et al., 1998). It has been shown that some IAA-amino acid conjugates also undergo oxidation. In vivo administration experiments demonstrated that IAA-Asp (**2**) was metabolized to OxIAA-Asp (**7**), without prior hydrolysis to free IAA (**1**), in several plant species (Östin et al., 1995, 1998). Furthermore, the formation of an OxIAA conjugate with a hexose was observed when IAA (**1**) was administered to *Arabidopsis* seedlings (Östin et al., 1998). Although the oxidative metabolism of IAA (**1**) is generally recognized to occur ubiquitously in plants, the amount of information available is relatively limited and so endogenous levels of the metabolites or their significance under normal growth conditions have not been well investigated. It is likely that some other metabolites are present at very low concentrations, but have an important role in the metabolism of IAA (**1**). Such metabolites could include oxidized IAA-amino acids that have not been detected in unoxidized forms in plants. If so, the presence of amino acid conjugation pathways predicted by the above-mentioned molecular biology study will be demonstrated.

In this study, we searched for new IAA metabolites in vegetatively growing *Arabidopsis*, focusing on those produced by oxidative processes. We used tandem mass spectrometry to develop a multiple reaction monitoring (MRM)-based method of screening that allowed for the selective and sensitive detection of oxidized IAA conjugates. Conjugates of 6-hydroxy-IAA were identified, thereby demonstrating for the first time the occurrence of hydroxylation at position C-6 in the indole ring of IAA (**1**) in plants. The results also suggest that previously undescribed conjugates of IAA (**1**) with Phe and Val are formed endogenously in *Arabidopsis*. In addition, we revealed that the OxIAA conjugate with glucose was present at high levels in seedlings, indicating that the formation of this metabolite was a predominant process in the catabolism of IAA (**1**) in *Arabidopsis*.

## 2. Results

### 2.1. Strategy for detecting IAA metabolites

In this study, we attempted to detect all oxidative metabolites of IAA (**1**) present in vegetatively growing *Arabidopsis*, using LC-ESI-MS/MS. For this purpose, we first studied the typical mass spectroscopic fragmentation of amide- and ester-conjugates of IAA (**1**) or oxidized IAA using synthetic model compounds, OxIAA-Asp (**7**), OxIAA-Glu (**8**), and IAA-Glc (**9**). By the product ion scan of ESI-MS/MS, OxIAA-Asp (**7**) was observed to yield a 2-oxoquinolinium ion at *m/z* 146 from the protonated molecule at *m/z* 307 $[M+H]^+$ in the positive mode, and an ion at *m/z* 132 from deprotonated molecule at *m/z* 305 $[M-H]^-$ in the negative mode by the neutral loss of the 2-oxoindole-3-acety moiety (174 amu), with relatively high intensity. In the case of OxIAA-Glu (**8**), the same fragmentation processes were observed, where an ion at *m/z* 146 was formed from the protonated molecule at *m/z* 321 $[M+H]^+$ in the positive mode, and an ion of $[M-174]^-$ at *m/z* 146 from *m/z* 319 $[M-H]^-$ in the negative mode. Thus, we deemed these two types of fragmentation processes typical of amide conjugates of oxidized IAA so applicable to the screening of relevant metabolites in the plant extracts by LC-ESI-MS/MS.

The synthetic IAA-Glc (**9**) afforded a deprotonated molecule at *m/z* 336 $[M-H]^-$ in the negative mode, which yielded the characteristic fragment ions at *m/z* 174 and 130 with the loss of the glucosyl moiety and by the decomposition into a quinolinium ion, respectively. Therefore, we assumed that an ester conjugate of oxidized IAA should yield ions of *m/z* 190 and 146 in high abundance under the same MS/MS conditions.

Based on these results, we established screening methods for the amide- and ester-type conjugates of oxidized IAA in the extract of *Arabidopsis*. In order to detect the amide-type conjugates, the extract was subjected to HPLC and the eluate was monitored using the MRM mode of MS/MS. Two sets of experiments were done for each extract, in which the ions that cleaved into fragments with *m/z* values of 146 and M−173 were detected, respectively. When an ion with the specified *m/z* value provided peaks with the identical retention times on the two chromatograms obtained under these two different sets of conditions, the ion was deemed possibly to be that of an amide-type conjugate of oxidized IAA. Likewise, the ester-type conjugates were searched for by combining the MS/MS detection methods that focus on the ions cleaved into those with *m/z* values of 146 and 190. Optimized parameters for MS/MS to monitor these transitions are listed in Table 1.

Table 1
Multiple reaction monitoring (MRM) parameters to detect IAA metabolites

| Target compounds | | Filtered ions | | DP (V) | FP (V) | EP (V) | CE (V) | CXP (V) |
|---|---|---|---|---|---|---|---|---|
| | | Q1 | Q3 | | | | | |
| OxIAA-amide | 1 | $[M+H]^+$ | *m/z* 146 | 71 | 290 | 10 | 33 | 8 |
| 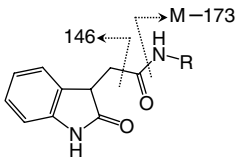  | 2 | $[M-H]^-$ | M−173 | −56 | −300 | −10 | −28 | −15 |
| OxIAA-ester | 1 | $[M-H]^-$ | *m/z* 190 | −41 | −250 | −10 | −16 | −19 |
| 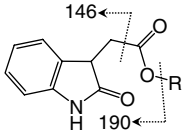  | 2 | $[M-H]^-$ | *m/z* 146 | −31 | −230 | −10 | −36 | −13 |

Q1, quadrupole 1; Q3, quadrupole 3; DP, declustering potential; FP, focusing potential; EP, entrance potential; CE, collision energy; CXP, collision cell exit potential.

### 2.2. Detection of novel metabolites

A LC-MRM-based search for oxidized IAA-conjugates with a molecular mass ranging from 200 to 1000 was performed. After the extract of 2-week-old plants was separated into six fractions by preparative HPLC, individual fractions were subjected to analysis. Five possible peaks, **I**–**III** from fraction 3, and **IV** and **V** from fraction 5, were found.

Peaks **I** ($t_R$, 6.2 min), **II** (6.4 min), and **III** (6.9 min) were detected as a result of the screening of ester conjugates of oxidized IAA, and the molecular weights of their components were all estimated to be 353 (Fig. 2a). The product ion spectra of these components were also identical, suggesting that the three are isomers. Furthermore, the fragmentation pattern of each component, in which ions were abundant at *m/z* 230, 190, 172, and 146, was similar to that of the glucose conjugate of IAA, **9**, in ESI-MS/MS, but the respective fragment ions were larger by 16 mass units (Fig. 2a). Thus, each compound in peaks **I**–**III** was thought to be a glucose conjugate of oxidized IAA.

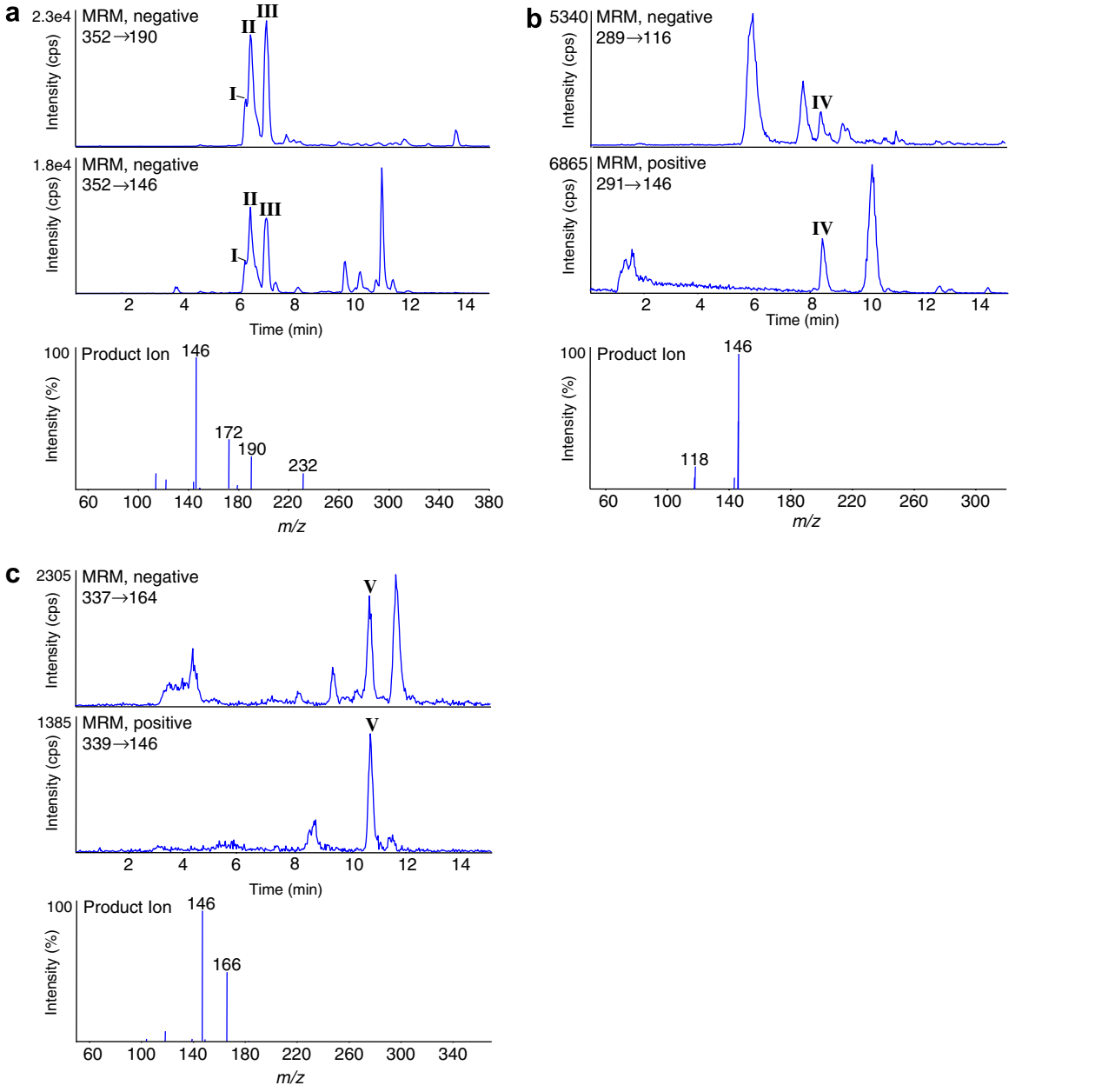


Fig. 2. LC-ESI-MS/MS-based screening of oxidized IAA metabolites in *Arabidopsis* extracts. The HPLC effluent was monitored by MS/MS in the MRM mode. (a) Peaks **I** ($t_R$, 6.2 min), **II** (6.4 min), and **III** (6.9 min) were detected as those of ester conjugates of oxidized IAA. The product ion spectrum for the deprotonated molecule of **III** is shown in the bottom. Components in **I**–**III** afforded almost the same spectra. (b and c) Peaks **IV** ($t_R$, 8.4 min) and **V** (10.5 min) were detected as those of amide conjugates of oxidized IAA. The product ion spectra for the protonated molecules are shown in the bottom, respectively.

The compound in peak **IV** ($t_R$, 8.4 min) was found during the screening of amide conjugates of oxidized IAA. Its molecular weight of was presumed to be 290 and the product ion spectrum is shown in Fig. 2b. The fragment ion at $m/z$ 118 was produced from the protonated molecule $[M+H]^+$ in the positive mode, while that at $m/z$ 116 was produced from the deprotonated molecule $[M-H]^-$ in the negative mode (data not shown), both of which were assigned to the ions related to the Val moiety in the compound formed by the cleavage of the amide bond. We presumed, therefore, that compound in **IV** was a Val conjugate of oxidized IAA.

The compound in peak **V** ($t_R$, 10.5 min) was also considered to be an amide conjugate, with a molecular weight of 338 (Fig. 2c). A product ion scan of compound **V** showed that the ions were obtained in abundance at $m/z$ 293 and 164 from the deprotonated molecule $[M-H]^-$ in the negative mode (data not shown) and at $m/z$ 166 and 146 from the protonated molecule $[M+H]^+$ in the positive mode (Fig. 2c). These spectra were well explained by assuming compound in **V** to be oxidized IAA linked to Phe.

### 2.3. Identification of compounds in peaks *I–V*

As indicated in the previous section, compounds in **I–III** were presumed to be glucose conjugates of oxidized IAA. Because of the presence of OxIAA (**6**) as an oxidative metabolite of IAA (**1**) in a variety of plant species (Normanly, 1997), we assumed that they were most likely to be 1-*O*-β-D-glucose esters of **2**. In order to confirm this, an authentic sample of OxIAA-Glc (**10**) was chemically synthesized from OxIAA (**6**) according to the method used for IAA-Glc (**9**) (Fig. 3a). Synthetic OxIAA-Glc (**10**) was identical with compound of **III** with respect to its chromatographical behavior and MS fragmentation pattern in LC-ESI-MS/MS (Table 2). The characteristic product ions were appropriately assigned as shown in Fig. 4. It was found that synthetic OxIAA-Glc (**10**) was gradually converted into a mixture of compounds in aqueous solution at room temperature, and the newly produced compounds had the same retention times ($t_R$, 6.2 and 6.4 min) as compounds in **I** and **II** (data not shown). This indicates that they are the isomers of OxIAA-Glc (**10**) presumably formed by keto-enol tautomerism and/or acyl migration.

The mass spectrum of compound in **IV** suggested that it was the Val conjugate of oxygenated IAA. However, its LC retention time was not identical with that of synthetic OxIAA-Val (**11**). Therefore, it was assumed that compound in **IV** had an oxidized indole moiety of IAA (**1**) that distinguished it from 2-oxoindole of OxIAA (**6**). In order to determine the oxidized position of the indole ring, a series of Val conjugates of hydroxy IAA (OH-IAA), i.e. 4-OH-IAA (**15**), 5-OH-IAA (**16**), 6-OH-IAA (**17**) and 7-OH-IAA (**18**), were synthesized from the corresponding methoxyindoles (**19**) (Fig. 3b). The structures of the synthetic compounds were confirmed by NMR spectroscopy and mass spectrometry. Among the synthetic standards, compound in **IV** agreed with 6-OH-IAA-Val (**13**) in terms of retention time and product ion spectra in LC-ESI-MS/MS (Table 2). Proposed assignments of characteristic product ions are shown in Fig. 4.

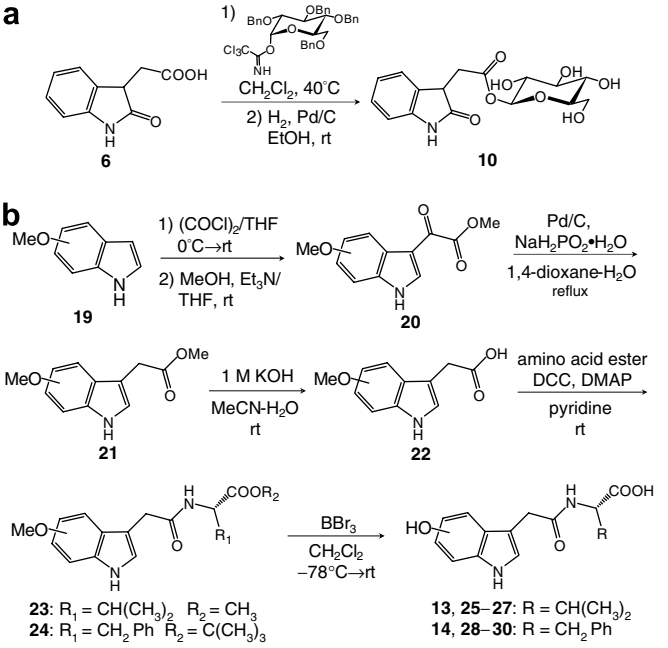


Fig. 3. Schemes of the synthesis of OxIAA-Glc (**10**) (a) and OH-IAA-Val (**13**, **25**–**27**) and OH-IAA-Phe (**14**, **28**–**30**) (b). For details, see Section 5. Pd/C, palladium on activated charcoal; EtOH, ethanol; $(COCl)_2$, oxalyl dichloride; THF, tetrahydrofuran; $Et_3N$; triethylamine; DCC, *N*,*N*′-dicyclohexylcarbodiimide; DMAP, 4-dimethylaminopyridine; $BBr_3$, boron tribromide; rt, room temperature.

Table 2
Tabulated LC-ESI-MS/MS-based analytical data of synthetic compounds

| Compound | Retention time (min) | Precursor ion ($m/z$) | Ions ($m/z$) (abundance) |
|---|---|---|---|
| **10** | 6.9 | 352 | 232 (2), 190 (9), 172 (15), 146 (100), 144 (24), 128 (27) |
| **13** | 8.4 | 291 | 146 (100), 118 (2), 72 (21) |
| **14** | 10.5 | 339 | 166 (1), 146 (100), 120 (28) |

Similarly, compound in **V** was also considered to be OH-IAA conjugated with Phe via an amide bond. To clarify its structure, a series of Phe conjugates of OH-IAA were synthesized (Fig. 3b), and their chromatographic behaviors as well as product ion spectra were compared with those of compound in **V** by LC-ESI-MS/MS (Table 2, Fig. 4). Consequently, compound in **V** was identified as 6-OH-IAA-Phe (**14**).

### 2.4. Administration studies for elucidating the biosynthetic route of oxidized IAA conjugates

#### 2.4.1. OxIAA-Glc (*10*)

It has been demonstrated that a hexose conjugate of OxIAA (**6**) was synthesized in plants administered IAA

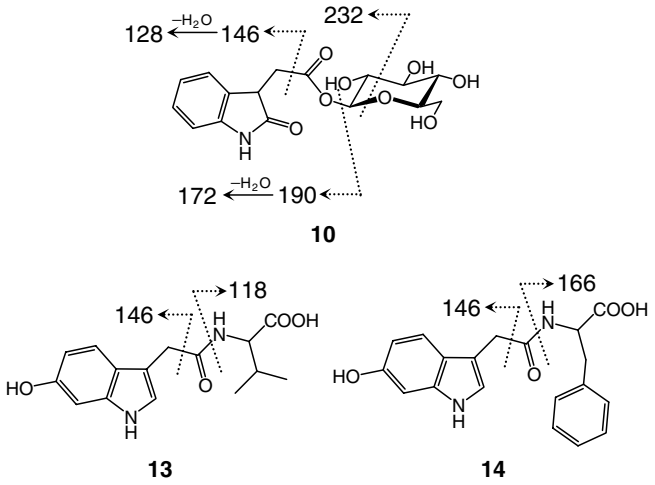


Fig. 4. Proposed MS fragmentation of OxIAA-Glc (**10**), 6-OH-IAA-Val (**13**), and 6-OH-IAA-Phe (**14**) in LC-ESI-MS/MS. Values represent *m*/*z* recorded.

(**1**) and OxIAA (**6**), and therefore, the conjugate is most likely synthesized by the oxidation of IAA (**1**) to OxIAA (**6**) and subsequent coupling with the hexose moiety (Östin et al., 1998). However, the hexose moiety has not been well characterized chemically. Besides, another reaction sequence, i.e. conjugation followed by oxidation, is still possible. To elucidate the biosynthetic route for OxIAA-Glc (**10**), we prepared two kinds of deuterium-labeled putative precursors, [2′,2′-$^2H_2$]IAA-Glc (**9**-$d_2$) and [2′,2′-$^2H_2$]OxIAA (**6**-$d_2$), and separately fed them to 2-week-old *Arabidopsis* plants grown in agar-solidified MS media. After incubation for 48 h in the dark, a significant incorporation of deuterium into OxIAA-Glc (**10**) from both precursors was observed by LC-ESI-MS/MS, which failed to discriminate the two possible routes (Fig. 5a and b). However, it was also observed that a substantial amount of deuterium-labeled IAA-Glc (**9**-$d_2$) underwent hydrolysis and the produced [2′,2′-$^2H_2$]IAA (**1**-$d_2$) was subsequently oxidized to [2′,2′-$^2H_2$]OxIAA (**6**-$d_2$) in *Arabidopsis* under the experimental conditions employed (data not shown). This suggests that OxIAA-Glc (**10**) is more likely synthesized via glucosylation of OxIAA (**6**) in *Arabidopsis*.

#### 2.4.2. 6-OH-IAA-Val (13) and 6-OH-IAA-Phe (14)

Amino acid conjugates of 6-OH-IAA (**17**) were considered to be biosynthesized either by oxidation of the corresponding IAA-amino acids, or by conjugation of 6-OH-IAA (**17**). In order to clarify this issue, deuterium-labeled IAA-Val (**4**), IAA-Phe (**5**), and 6-OH-IAA (**17**) were, respectively, administered to 2-week-old plants grown in MS agar media for 48 h. The formation of 6-OH-IAA-amino acids from supplied IAA-amino acids was confirmed by using LC-ESI-MS/MS, where the peaks with expected mass spectroscopic properties were detected in the MRM mode with identical retention times to those of synthetic standards (Fig. 5c and d). The structural identity of the component in each peak was also confirmed by its product-ion spectrum. On the other hand, exogenous 6-OH-IAA (**17**) was not incorporated into the amino-acid conjugates to a measurable extent (data not shown). We concluded, therefore, that 6-OH-IAA-Val (**13**) and 6-OH-IAA-Phe (**14**) were synthesized by hydroxylation of IAA-Val (**4**) and IAA-Phe (**5**) at the 6-position of the indole moiety, respectively.

In these experiments, the formation of OxIAA-Val (**11**) ($t_R$, 10.7 and 11.3 min) and OxIAA-Phe (**12**) ($t_R$, 12.6 and 13.0 min) was also observed after administration of deuterium-labeled IAA-Val (**4**-$d_2$) and IAA-Phe (**5**-$d_2$), respectively (Fig. 5c and d), although these conjugates have never been detected in intact plants. The ion intensities of these conjugates were higher than those of conjugates of 6-OH-IAA (**17**). It is likely that supplied IAA-amino acids are more susceptible to oxidation at position C-2 of the indole ring to form OxIAA-amino acids, rather than that at C-6, although the physiological importance of this conversion in *Arabidopsis* under normal conditions remains unknown.

### 2.5. Root growth inhibition assay

To examine the auxin-activity of 6-OH-IAA (**17**) and its conjugates (**13**, **14**), we carried out a biological assay in terms of the inhibition of root growth in *Arabidopsis* seedlings (Staswick et al., 2005). None of the compounds tested showed significant activity (Fig. 6), indicating that 6-hydroxylation, as well as 2-oxidation, of the indole ring is an inactivation process for IAA (**1**).

### 2.6. Quantitative analysis of IAA metabolites

The levels of oxidative IAA metabolites in *Arabidopsis* seedlings at 7 and 14 days after germination (DAG) were determined by LC–MS/MS. The MRM parameters for the analyses are listed in Table 3. Of seven metabolites quantified, OxIAA-Glc (**10**) was found in the largest amount (1.95 and 1.53 pmol $g^{-1}$ fresh wt. at 7 and 14 DAG, respectively, Table 4). The amounts of free IAA (**1**), OxIAA (**6**), and IAA-Glc (**9**) were almost the same, while those of IAA-Asp (**2**) and IAA-Glu (**3**) were in the range of 1/8–1/3 of the level of free IAA (**1**). The amounts of 6-OH-IAA-Val (**13**) and 6-OH-IAA-Phe (**14**) were under the detection limit at 7 DAG. In 14-day-old *Arabidopsis*, 6-OH-IAA-Val (**13**) and 6-OH-IAA-Phe (**14**) were present at 11 and 2 pmol $g^{-1}$ fresh wt, respectively (Table 4). These levels were considerably low, compared to those of IAA (**1**) and other metabolites.

## 3. Discussion

Conjugation represents a major part of IAA (**1**) metabolism in plants. In particular, more than 98% of total IAA (**1**) in *Arabidopsis* seedlings is estimated to be present as conjugated forms, most of which remain chemically

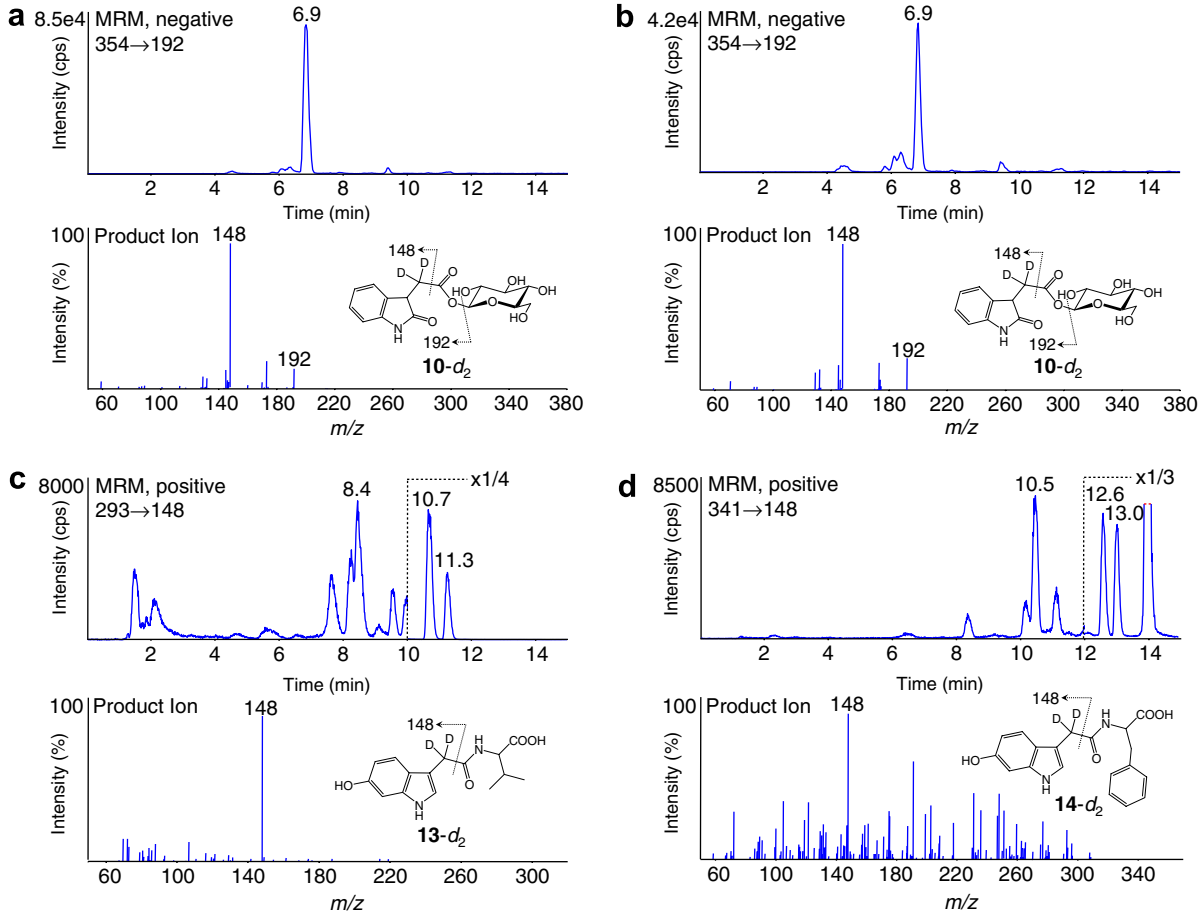


Fig. 5. Administration of deuterium-labeled IAA metabolites to *Arabidopsis* plants grown in MS media. [2′,2′-$^2H_2$]IAA-Glc (**9**-$d_2$) (a) and [2′,2′-$^2H_2$]OxIAA (**6**-$d_2$) (b) were incorporated into OxIAA-Glc (**10**) ($t_R$, 6.9 min). [2′,2′-$^2H_2$]IAA-Val (**4**-$d_2$) (c) and [2′,2′-$^2H_2$]IAA-Phe (**5**-$d_2$) (d) were incorporated into 6-OH-IAA-Val (**13**) ($t_R$, 8.4 min) and 6-OH-IAA-Phe (**14**) (10.5 min), respectively. Deuterium-incorporation was confirmed by comparing each product ion spectrum with that of synthetic deuterium-labeled standard.

uncharacterized (Tam et al., 2000; Ljung et al., 2002). In order to further elucidate the metabolism of IAA (**1**) in *Arabidopsis*, we first searched for novel IAA conjugates in the vegetative tissue using LC-ESI-MS/MS. Although the method used was designed to detect any conjugates present in a certain amount, no novel conjugate was found in the soluble form (data not shown), and therefore, it is unlikely that some kind of conjugate with a relatively simple structure accounts for the hitherto uncharacterized metabolites that are hydrolyzed to afford IAA (**1**). Subsequently, we changed our objective and searched for the IAA conjugates that underwent oxidation. It has been shown that IAA-Asp (**2**) is oxidized to OxIAA-Asp (**7**) in several plant species (Östin et al., 1995, 1998). We speculated that oxidation of IAA-conjugates would also make an important contribution to the regulation of their levels *in planta*. Thus, we developed a LC-ESI-MS/MS-based method to screen for oxidized IAA conjugates in *Arabidopsis*. In general, two modes of MS/MS; the precursor ion scan and neutral loss scan, are used for structure-based searches of metabolites. Preliminary experiments revealed that these scan methods were not sensitive enough to detect metabolites present in minute amounts. Therefore, we employed the MRM mode to detect sensitively and selectively oxidative IAA conjugates with a molecular weight

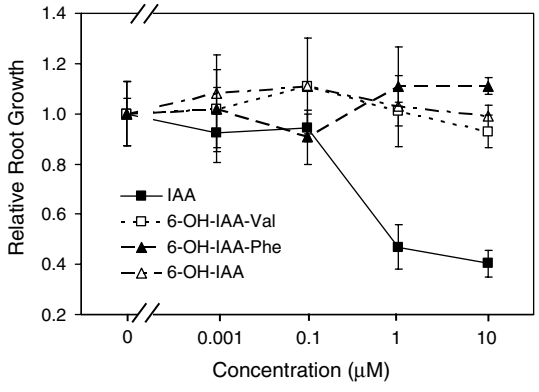


Fig. 6. Effect of IAA (**1**), 6-OH-IAA-Val (**13**), 6-OH-IAA-Phe (**14**), and 6-OH-IAA (**17**) on inhibition of the root growth of *Arabidopsis* seedlings. Four-day-old seedlings were transferred on MS media containing each compound, and incubated vertically for 5 days. Values shown are means ± SD from five measurements.

Table 3
Multiple reaction monitoring (MRM) parameters to quantify IAA (**1**) and metabolite

| Compounds | Polarity | Filtered ions (*m/z*) | | DP (V) | FP (V) | EP (V) | CE (V) | CXP (V) |
|---|---|---|---|---|---|---|---|---|
| | | Q1 | Q3 | | | | | |
| IAA (**1**) | Positive | 176 | 130 | 40 | 370 | 10 | 19 | 7.5 |
| [$^{13}C_6$]IAA ([$^{13}C_6$]-**1**) | Positive | 182 | 136 | 40 | 370 | 10 | 19 | 7.5 |
| IAA-Asp (**2**) | Positive | 291 | 130 | 46 | 340 | 10 | 25 | 8 |
| [2′,2′-$^2H_2$]IAA-Asp (**2**-$d_2$) | Positive | 293 | 132 | 46 | 340 | 10 | 25 | 8 |
| IAA-Glu (**3**) | Positive | 305 | 130 | 21 | 260 | 10 | 27 | 8 |
| [2′,2′-$^2H_2$]IAA-Glu (**3**-$d_2$) | Positive | 307 | 132 | 21 | 260 | 10 | 27 | 8 |
| IAA-Glc (**9**) | Negative | 336 | 174 | −51 | −260 | −10 | −14 | −11 |
| [2′,2′-$^2H_2$]IAA-Glc (**9**-$d_2$) | Negative | 338 | 176 | −51 | −260 | −10 | −14 | −11 |
| OxIAA (**6**) | Positive | 192 | 146 | 36 | 230 | 10 | 17 | 8 |
| [2′,2′-$^2H_2$]OxIAA (**6**-$d_2$) | Positive | 194 | 148 | 36 | 230 | 10 | 17 | 8 |
| OxIAA-Glc (**10**) | Negative | 352 | 190 | −46 | −300 | −10 | −24 | −11 |
| [2′,2′-$^2H_2$]OxIAA-Glc (**10**-$d_2$) | Negative | 354 | 192 | −46 | −300 | −10 | −24 | −11 |
| 6-OH-IAA-Val (**13**) | Positive | 291 | 146 | 30 | 200 | 10 | 30 | 15 |
| [2′,2′-$^2H_2$]6-OH-IAA-Val (**13**-$d_2$) | Positive | 293 | 148 | 30 | 200 | 10 | 30 | 15 |
| 6-OH-IAA-Phe (**14**) | Positive | 339 | 146 | 30 | 200 | 10 | 30 | 15 |
| [2′,2′-$^2H_2$]6-OH-IAA-Phe (**14**-$d_2$) | Positive | 341 | 148 | 30 | 200 | 10 | 30 | 15 |

Q1, quadrupole 1; Q3, quadrupole 3; DP, declustering potential; FP, focusing potential; EP, entrance potential; CE, collision energy; CXP, collision cell exit potential.

Table 4
Quantitative analysis of IAA (**1**) and its metabolites in 7- and 14-day-old *Arabidopsis*

| Sample | IAA (**1**) | IAA-Asp (**2**) | IAA-Glu (**3**) | IAA-Glc (**9**) | OxIAA (**6**) | OxIAA-Glc (**10**) | 6-OH-IAA-Phe (**13**) | 6-OH-IAA-Val (**14**) |
|---|---|---|---|---|---|---|---|---|
| DAG | pmol $g^{-1}$ fresh wt. | | | | | | | |
| 7 | 69 ± 10 | 13 ± 2.8 | 7.8 ± 0.8 | 58 ± 18 | 63 ± 17 | 1950 ± 544 | –[a] | – |
| 14 | 38 ± 8 | 12 ± 0.8 | 13 ± 0.1 | 41 ± 12 | 47 ± 9 | 1530 ± 73 | 11 ± 1.3 | 2 ± 0.5 |

Data shown are means ± SD of three replicates.
[a] Below the quantification limit.

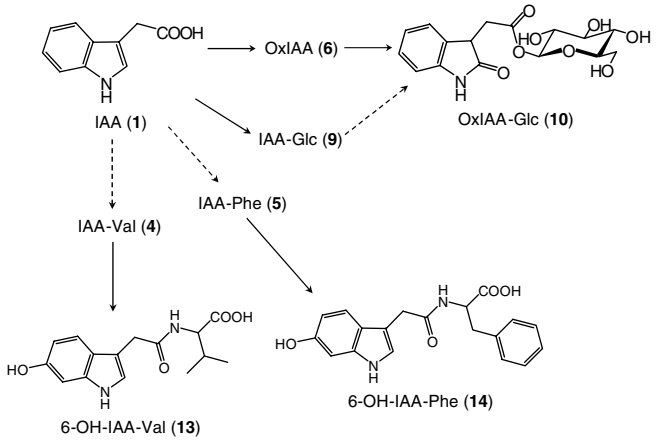


Fig. 7. Metabolic pathways of IAA (**1**) in *Arabidopsis* seedlings showing the newly identified oxidative metabolites OxIAA-Glc (**10**), 6-OH-IAA-Val (**13**), and 6-OH-IAA-Phe (**14**). The solid arrows represent the steps that have been demonstrated in *Arabidopsis*.

ranging from 200 to 1000 in a more targeted manner. Conditions for detection were set based on the MS/MS data for synthetic model compounds as described above. As a consequence, we found three novel metabolites in the extract of *Arabidopsis* fractionated by preparative HPLC (Fig. 2).

Two amide-type conjugates, 6-OH-IAA-Val (**13**) and 6-OH-IAA-Phe (**14**), were identified for the first time as metabolites of IAA (**1**) in plants. The label-incorporation experiment showed that these compounds were synthesized from IAA-Val (**4**) and IAA-Phe (**5**) by hydroxylation at position C-6 of the indole ring, which represents a previously unknown pathway for the catabolism of IAA (**1**) (Fig. 5c and d). Although the presence of the precursors, IAA-Val (**4**) and IAA-Phe (**5**), has not been confirmed in intact plant tissues, IAA-Val (**4**) was reported as a metabolite of exogenous IAA (**1**) in the crown gall callus of *Parthenocissus tricuspidata* (Feung et al., 1976). In this case, however, whether IAA-Val (**4**) was of plant- or microbial-origin was not described. Recently, a family of *GH3* genes encoding a series of IAA-amide synthases was identified, and the in vitro translated protein was demonstrated to have activity to conjugate IAA (**1**) with Phe and Val (Staswick et al., 2005). Besides, an IAA-amide hydrolase, ILR1, expressed in *Escherichia coli* was most active against IAA-Phe (**5**) among a series of IAA-amino acids (Bartel and Fink, 1995). Together with these findings, the results of the present study strongly suggest that IAA-Val (**4**) and IAA-Phe (**5**) are certainly formed in *Arabidopsis*. Kowalczyk and Sandberg have demonstrated the existence of IAA-Ala and IAA-Leu in *Arabidopsis* seedlings (Kowalczyk and Sandberg, 2001). These amino acid conjugates have been considered as storage forms of auxin, since they have auxin activity after releasing free IAA (**1**) in vivo

when applied exogenously (Bartel and Fink, 1995; Davies et al., 1999; LeClere et al., 2002; Rampey et al., 2004). However, the actual levels of IAA-Ala and IAA-Leu in the tissue were quite low compared to the levels of other metabolites (Kowalczyk and Sandberg, 2001). It is likely that a rapid turnover of both IAA-Ala and IAA-Leu makes it difficult to detect these metabolites in the plant. This may also be the case with IAA-Val (**4**) and IAA-Phe (**5**). Although they have never been detected in plants, they could play an important role in regulating the level of free IAA (**1**).

Östin et al. investigated the metabolism of IAA (**1**) administered to *Arabidopsis* seedlings, in which three oxidative IAA-Asp were detected using LC-FAB (fast-atom bombardment)-MS (Östin et al., 1998). One of them was presumed to be IAA hydroxylated in the indole moiety based on the mass spectrum, whereas the others were identified as tautomers of OxIAA-Asp (**7**). In the present study, however, no data were obtained to suggest the presence of OH-IAA-Asp. Chances are small that OH-IAA-Asp was lost during the sample pretreatment procedure employed in this study, because we succeeded in detecting a predicted OH-IAA-Asp of similar polarity in rice plants using the same procedure (unpublished data). It is likely that the formation of OH-IAA-Asp is a specific response to the exogenous IAA (**1**) in *Arabidopsis*, and its level in the intact tissue is quite low.

No enzymes or genes have been implication in hydroxylating the indole moiety of IAA (**1**) in plants. In this relation, a gene referred to as *iar1* was isolated from an *Arabidopsis* mutant, which suggested the presence of a genetically controllable oxidation system for IAA (**1**) (Lasswell et al., 2000). This gene confers insensitivity to the growth inhibition caused by amino acid conjugates of IAA (**1**), but has no effect on sensitivity to IAA (**1**). The gene also has some homology with Drosophila Catsup protein, considered to be a negative regulator of the conversion of L-tyrosine to 3,4-dihydroxy-L-phenylalanine (DOPA) (Kumer and Vrana, 1996). By analogy, IAR1 was speculated to negatively regulate the hydroxylation of the indole-moiety of IAA-amino acids. The mutation of *IAR1* should result in the catabolism of IAA-amino acids by hydroxylation, which would account for the insensitivity of the mutant to exogenous IAA-amino acids without any effect on the sensitivity to IAA (**1**). This hypothesis, however, is still lacking in many respects, and requires further examination, together with the biochemical evidence for the presence of hydroxylation activity toward IAA (**1**). A detailed analysis of OH-IAA-amino acids in the *iar1* mutant would provide more information.

As shown in Fig. 6, 6-OH-IAA (**17**) and its amino-acid conjugates (**13**, **14**) showed no inhibition of the root growth of *Arabidopsis*. This indicates that the 6-hydroxylation of the indole ring is an inactivation process for IAA-amino acids. The amino acid conjugates of 6-OH-IAA (**17**) are relatively unstable. In fact, we observed that authentic samples of 6-OH-IAA conjugates (**13**, **14**) gradually decomposed in the standard solution during the LC-ESI-MS/MS analysis. Thus, **13** and **14** are likely to be further transformed in plants. Clarifying the fate of these compounds is also interesting and important to complete understanding the metabolism of IAA (**1**).

As a result of screening ester-conjugates of oxidized IAA, we found a new endogenous metabolite, OxIAA-Glc (**10**) (Fig. 2a), whose structure was confirmed by comparison with a synthetic standard (Table 2). It has been reported that OxIAA-hexose was produced after the application of IAA (**1**) in *Arabidopsis*, but no detailed structural characterization was conducted for the hexose moiety of this metabolite (Östin et al., 1998). Since no OxIAA-hexose other than OxIAA-Glc (**10**) was detected in the present study (Fig. 2a), OxIAA-Glc (**10**) is considered to account for the previously detected OxIAA-hexose in *Arabidopsis*. By the isotope incorporation study with deuterium-labeled IAA-Glc (**9**-$d_2$) or OxIAA (**6**-$d_2$), it was confirmed that glucosylation of OxIAA (**6**) occurred in vivo (Fig. 5a and b). However, the presence of an oxidation pathway for IAA-Glc (**9**) was not confirmed in this study. Administration experiments using IAA-Glc (**9**) with an isotope-label in the Glc moiety may help to elucidate the major pathway in plants. To date, a gene product of UGT84B1 has been identified as a glucosyltransferase that forms IAA-Glc (**9**) in *Arabidopsis* (Jackson et al., 2001). However, this enzyme has been shown to have no activity toward OxIAA (**6**), suggesting that a different enzyme is responsible for its glucosylation. Quantification of IAA metabolites showed that the level of OxIAA-Glc (**10**) was very high in *Arabidopsis* seedlings, 28–40 times that of free IAA (**1**), far above levels of the metabolites from which IAA (**1**) could reversibly be produced, namely IAA-Glc (**9**) (Table 4), IAA-Ala, and IAA-Leu (Kowalczyk and Sandberg, 2001). Since OxIAA-Glc (**10**) was inactive as an auxin and is unlikely to be reversibly converted to IAA (**1**), it is suggested that inactivation of IAA (**1**) occurs rather actively, and the formation of reserve IAA (**1**) may play a minor role in the regulation of IAA (**1**) levels in *Arabidopsis* seedlings. In other words, the level of IAA (**1**) may be mainly regulated in a relatively simple manner by the balance of biosynthesis and catabolic inactivation. The change in the content of each metabolite with the plant growth is of interest, and a potentially important subject of future study.

## 4. Concluding remarks

In conclusion, we have identified three new oxidative IAA metabolites, OxIAA-Glc (**10**), 6-OH-IAA-Val (**13**), and 6-OH-IAA-Phe (**14**) in *Arabidopsis* (Fig. 7). Among these, OxIAA-Glc (**10**) constituted the largest proportion of all the metabolites of IAA (**1**) in *Arabidopsis*. We also have demonstrated that hydroxylation at position C-6 of the IAA moiety of amino acid conjugates occurs as a novel catabolic pathway for IAA (**1**) by conducting feeding experiments in vivo. The result also provided substantial

evidence that IAA-Val (**4**) and IAA-Phe (**5**) are synthesized in *Arabidopsis* plants. Although peroxidases have been proposed to oxidize at C-2 of IAA (**1**) in vitro (Normanly, 1997), to our knowledge, little is known about the enzyme which catalyzes hydroxylation of the indole-ring in plants. Further detailed study will no doubt provide us new insight into the oxidative metabolism of IAA (**1**).

## 5. Experimental

### 5.1. Plant material

Seeds of *Arabidopsis thaliana* ecotype Columbia were surface sterilized in 5% (v/v) sodium hypochlorite containing 0.05% (v/v) Tween 20 for 5 min, and then washed three times with sterile $H_2O$. Seeds were germinated in petri dishes containing agar-solidified MS medium and were grown at 22 °C with 16-h photoperiods.

### 5.2. Synthesis of OxIAA-Asp (7), OxIAA-Glu (8), and IAA-Glc (9)

OxIAA (**6**) was synthesized from IAA (**1**) according to the method of Tuominen et al. with some modifications (Tuominen et al., 1994). OxIAA-Asp (**7**) and OxIAA-Glu (**8**) were synthesized by condensing OxIAA (**6**) with the corresponding L-amino acid *t*-butyl ester HCl using *N*,*N*′-dicyclohexylcarbodiimide (DCC) and 4-dimethylaminopyridine (DMAP) in pyridine at room temperature, overnight, followed by acidic hydrolysis [trifluoroacetic acid–triisopropylsilane–$H_2O$ (95:2.5:2.5, v/v), room temperature, 1 h]. The yields of OxIAA-Asp (**7**) and OxIAA-Glu (**8**) were 54% and 66%, respectively. IAA-Glc (**9**) was synthesized from IAA (**1**) according to the method of Schmidt et al. with some modifications (Schmidt and Michel, 1985).

### 5.3. LC-MRM-MS/MS-based screening of oxidative IAA conjugates

Two-week-old *Arabidopsis* plants (4.7 g fresh wt.) were homogenized in liquid $N_2$ and immediately soaked in acetone–$H_2O$ (4:1, v/v) containing 2.5 mM diethyldithiocarbamic acid. After repeating the extraction procedure, the extract was concentrated under reduced pressure. The aqueous concentrate was acidified to pH 3.0 and passed through a Sep-Pak Plus C18 cartridge (Waters, Massachusetts, USA), and then eluted with $CH_3CN$–$H_2O$ (3:2, v/v). The eluate was concentrated under reduced pressure and dissolved in $CH_3CN$–$H_2O$ (1:1, v/v, 400 μl). The sample was fractionated on a preparative HPLC system (Shimadzu, Kyoto, Japan). For elution, a gradient from $CH_3CN$–$H_2O$ containing 0.05% (v/v) AcOH (1:9, v/v) to $CH_3CN$–$H_2O$ containing 0.05% (v/v) AcOH (9:1, v/v) over 30 min, with a flow rate of 3.2 ml/min was used. An Inersil ODS-3 column (250 mm × 10 mm, GL Science, Tokyo, Japan) was used. Six fractions were collected every 5 min. The samples were dissolved in 200 μl of an appropriate concentration of MeCN.

Screening of oxidative-IAA conjugates was performed using a LC-ESI-MS/MS system, consisting of an Agilent 1100 HPLC system coupled to an API3000 triple-quadrupole-stage mass spectrometer (Applied Biosystems/MDS Sciex, Ontario, Canada). A Cadenza CD-C18 column (75 mm × 2 mm, Imtakt, Kyoto, Japan) was used. The mobile phase was delivered at a flow rate of 200 μl/min with an initial mixture of MeOH–$H_2O$ containing 0.05% (v/v) AcOH (1:4, v/v) for 3 min, followed by a 12-min linear increase to MeOH–$H_2O$ containing 0.05% (v/v) AcOH (4:1, v/v). The temperature was 30 °C. The parameters for the screening of metabolites were optimized using synthetic OxIAA-Asp (**7**) and IAA-Glc (**9**). A MRM-based screening of metabolites in the range from *m*/*z* 200 to 1000 was performed. Product-ion-scan analyses of metabolites were carried out under the same LC conditions. The data obtained were processed with Analyst 1.3 software (Applied Biosystems).

### 5.4. Synthesis of OxIAA-Glc (10), OxIAA-Val (11), OxIAA-Phe (12), OH-IAA-Val (13, 25–27), and OH-IAA-Phe (14, 28–30)

$^1H$ and $^{13}C$ NMR spectra were obtained using a Bruker Avance 400 NMR spectrometer with tetramethylsilane as an internal standard. Mass spectra were recorded with an API3000 mass spectrometer as described above.

*OxIAA-Glc (10)*. OxIAA-Glc (**10**) was synthesized from OxIAA (**6**) using the same procedure as for IAA-Glc (**9**). $^1H$ NMR (400 MHz, $CD_3OD$): $\delta$ 2.82–2.92 (1H, *m*), 3.08–3.19 (1H, *m*), 3.31–3.45 (4H, *m*), 3.60–3.84 (3H, *m*), 5.48 (0.5H, *d*, $J = 8.1$ Hz), 5.53 (1H, *d*, $J = 8.1$ Hz), 6.90 (1H, *d*, $J = 7.7$ Hz), 6.98 (1H, *dd*, $J = 7.5$, 7.6 Hz), 7.20 (1H, *t*, $J = 7.7$ Hz), 7.29 (1H, *d*, $J = 7.4$ Hz). $^{13}C$ NMR (100 MHz, $CD_3OD$): $\delta$ 35.31, 35.43, 62.24, 70.92, 73.83, 73.89, 77.7, 77.75, 78.69, 78.75, 95.97, 96.03, 110.85, 110.87, 123.33, 123.38, 125.25, 129.26, 129.29, 130.16, 130.20, 143.55, 143.62, 176.49, 181.06, 181.11. MS (ESI): *m*/*z* 354 $[M+H]^+$.

*OxIAA-Val (11)*. OxIAA-Val (**11**) was synthesized using the same procedure as for OxIAA-Asp (**7**) in 78% yield. $^1H$ NMR (400 MHz, $CD_3OD$): $\delta$ 0.78–0.91 (3H, *m*), 0.94–0.99 (3H, *m*), 2.16 (1H, *m*), 2.67 (1H, *m*), 3.01 (1H, *m*), 4.30 (0.5H, *d*, $J = 5.5$ Hz), 4.35 (0.5H, *d*, $J = 5.5$ Hz), 6.88 (1H, *m*), 6.96 (1H, *m*), 7.17–7.25 (2H, *m*). $^{13}C$ NMR (100 MHz, $CD_3OD$): $\delta$ 18.5, 19.5, 31.6, 37.0, 59.1, 110.8, 123.2, 125.4, 129.2, 130.5, 143.6, 174.7. MS (ESI): *m*/*z* 291 $[M+H]^+$.

*OxIAA-Phe (12)*. OxIAA-Phe (**12**) was synthesized the same as OxIAA-Asp (**7**) in 77% yield. $^1H$ NMR (400 MHz, $CD_3OD$): $\delta$ 2.42–2.58 (1H, *m*), 2.84–2.96 (2H, *m*), 3.14–3.27 (1H, *m*), 3.72–3.77 (1H, *m*), 4.69 (0.5H, *dd*, $J = 5.2$, 8.8 Hz), 4.78 (0.5H, *dd*, $J = 4.7$, 9.5 Hz), 6.79 (0.5H, *d*, $J = 7.4$ Hz), 6.82–6.87 (1H, *m*), 6.92 (0.5H, *dd*, $J = 7.5$ Hz), 7.12–7.27 (7H, *m*). $^{13}C$ NMR (100 MHz,

$CD_3OD$): δ 36.92, 37.04, 38.31, 38.39, 43.78, 44.01, 55.08, 55.22, 110.74, 123.31, 123.45, 125.21, 125.42, 127.78, 129.01, 129.11, 129.42, 129.49, 130.19, 130.39, 130.51, 138.25, 138.40, 143.13, 143.25, 172.71, 174.56, 181.57. MS (ESI): *m/z* 321 $[M+H]^+$.

*OH-IAA-Val (**13**, **25**–**27**)*. The scheme for synthesizing 4-OH-, 5-OH-, 6-OH-, and 7-OH-IAA-Val (**25**, **26**, **13**, **27**) is shown in Fig. 3. Treatment of methoxyindole (**19**) with 1.1 equivalents of oxalyl dichloride at 0 °C for 2 h, and subsequently excess MeOH for 4 h gave methoxyindoleoxoacetic acid methyl ester (**20**) (4-MeO: 57%, 5-MeO: 95%, 6-MeO: 70%, 7-MeO: 87%). Reduction of α-ketone with 0.4 equivalents (w/w) of 10% (w/w) palladium on activated charcoal and 10 equivalents of $NaH_2PO_2 \cdot H_2O$ in 1,4-dioxane–$H_2O$ at room temperature for 2 days afforded methoxyindole-3-acetic acid methyl ester (MeO-IAA-OMe, **21**) (4-MeO: 83%, 5-MeO: 94%, 6-MeO: 74%, 7-MeO: 96%). Treatment of **21** with 1 M KOH in THF–$H_2O$ gave MeO-IAA (**22**) quantitatively. Condensation of **22** with L-valine methyl ester was conducted with DCC and DMAP in pyridine at room temperature overnight to give MeO-IAA-Val-OMe (**23**) quantitatively. Demethylation using four equivalents of boron tribromide in dichloromethane under Ar at −78 °C overnight afforded OH-IAA-Val (**25**: 38%, **26**: 33%, **13**: 26%, **27**: 47%). *4-OH-IAA-Val (**25**)*. $^1$H NMR (400 MHz, $CD_3CN$): δ 0.86 (3H, *d*, *J* = 7.1 Hz), 0.88 (3H, *d*, *J* = 7.0 Hz), 2.12 (1H, *m*), 3.74 (2H, *d*, *J* = 1.9 Hz), 4.29 (1H, *dd*, *J* = 5.4, 8.3 Hz), 6.43 (1H, *dd*, *J* = 1.0, 7.4 Hz), 6.91 (1H, *dd*, *J* = 1.0, 8.2 Hz), 6.97 (1H, *dd*, *J* = 7.5, 8.1 Hz), 7.03 (1H, *d*, *J* = 2.4 Hz), 7.25 (1H, *d*, *J* = 7.4 Hz), 9.10 (1H, *br. s*), 9.96 (1H, *br. s*). $^{13}$C NMR (100 MHz, $CD_3CN$): δ 18.0, 19.2, 31.2, 34.7, 58.5, 104.7, 106.5, 108.4, 123.3, 124.0, 139.9, 151.9, 172.6, 175.9. MS (ESI): *m/z* 291 $[M+H]^+$. *5-OH-IAA-Val (**26**)*. $^1$H NMR (400 MHz, $CD_3CN$): δ 0.79 (3H, *d*, *J* = 6.9 Hz), 0.86 (3H, *d*, *J* = 6.8 Hz), 2.10 (1H, *m*), 3.68 (2H, *s*) 4.31 (1H, *dd*, *J* = 5.4, 8.2 Hz), 6.70 (1H, *dd*, *J* = 2.3, 8.7 Hz), 6.82 (1H, *br. s*), 6.91 (1H, *d*, *J* = 2.2 Hz), 7.14 (1H, *d*, *J* = 2.1 Hz), 7.24 (1H, *d*, *J* = 8.7 Hz), 9.07 (1H, *br. s*). $^{13}$C NMR (100 MHz, $CD_3CN$): δ 1.79, 19.3, 31.2, 33.3, 58.6, 103.5, 108.2, 112.8, 113.0, 126.0, 128.8, 132.3, 151.4, 172.9 (2). MS (ESI): *m/z* 291 $[M+H]^+$. *6-OH-IAA-Val (**13**)*. $^1$H NMR (400 MHz, $CD_3CN$): δ 0.78 (3H, *d*, *J* = 6.9 Hz), 0.85 (3H, *d*, *J* = 6.9 Hz), 2.07 (1H, *m*), 3.63 (2H, *s*), 4.27 (1H, *dd*, *J* = 5.4, 8.4 Hz), 6.61 (1H, *dd*, *J* = 2.2, 8.5 Hz), 6.64 (1H, *d*, *J* = 9.0 Hz), 6.80 (1H, *d*, *J* = 2.2 Hz), 7.02 (1H, *d*, *J* = 2.3 Hz), 7.35 (1H, *d*, *J* = 8.5 Hz), 8.97 (1H, *br. s*). $^{13}$C NMR (100 MHz, $CD_3CN$): δ 1.80, 19.4, 31.2, 33.6, 58.4, 97.6, 109.5, 110.3, 120.2, 122.2, 123.5, 138.5, 154.1, 173.2, 173.4. MS (ESI): *m/z* 291 $[M+H]^+$. *7-OH-IAA-Val (**27**)*. $^1$H NMR (400 MHz, $CD_3CN$): δ 0.78 (3H, *d*, *J* = 6.9 Hz), 0.85 (3H, *d*, *J* = 6.9 Hz), 2.07 (1H, *m*), 3.65 (2H, *s*), 4.26 (1H, *dd*, *J* = 5.5, 8.4 Hz), 6.58 (1H, *dd*, *J* = 0.6, 7.5 Hz), 6.62 (1H, *br. s*), 6.88 (1H, *dd*, *J* = 7.7, 7.9 Hz), 7.08 (1H, *d*, *J* = 8.0 Hz), 7.14 (1H, *d*, *J* = 2.3 Hz), 9.18 (1H, *br. s*). $^{13}$C NMR (100 MHz, $CD_3CN$): δ 1.80, 19.4, 31.3, 33.6, 58.4, 107.1, 110.2, 111.6, 120.8, 124.6, 127.2, 130.3, 143.8, 173.2, 172.9. MS (ESI): *m/z* 291 $[M+H]^+$.

*OH-IAA-Phe (**14**, **28**–**30**)*. MeO-IAAs (**22**) were individually condensed with L-phenylalanine *t*-butyl ester in the presence of DCC and DMAP in pyridine at room temperature overnight to give MeO-IAA-Phe-*t*Bu (**24**) quantitatively. Deprotection with four equivalents of boron tribromide in $CH_2Cl_2$ under Ar at −78 °C for 4 h afforded OH-IAA-Phe (**28**: 57%, **29**: 70%, **14**: 43%, **30**: 27%). *4-OH-IAA-Phe (**28**)*. $^1$H NMR (400 MHz, $CD_3CN$): δ 2.95 (1H, *dd*, *J* = 7.6, 13.9 Hz), 3.10 (1H, *dd*, *J* = 5.3, 13.9 Hz), 3.67 (2H, *s*), 4.62 (1H, *m*), 6.43 (1H, *d*, *J* = 7.4 Hz), 6.90–6.98 (3H, *m*), 7.02–7.03 (2H, *m*), 7.09–7.14 (2H, *m*), 7.22 (1H, *d*, *J* = 7.5 Hz), 7.58 (1H, *s*), 9.11 (1H, *br. s*), 9.62 (1H, *br. s*). $^{13}$C NMR (100 MHz, $CD_3CN$): δ 34.7, 37.6, 54.6, 104.8, 106.5, 108.1, 123.5, 124.0, 127.7, 129.2 (2), 130.2 (2), 137.4, 139.9, 151.8, 172.4, 175.4. MS (ESI): *m/z* 339 $[M+H]^+$. *5-OH-IAA-Phe (**29**)*. $^1$H NMR (400 MHz, $CD_3CN$): δ 2.92 (1H, *dd*, *J* = 7.4, 13.9 Hz), 3.04 (1H, *dd*, *J* = 5.2, 13.9 Hz), 3.54 (2H, *s*), 4.60 (1H, *dt*, *J* = 5.2, 7.5 Hz), 6.53 (1H, *d*, *J* = 7.4 Hz), 6.71 (1H, *dd*, *J* = 2.2, 8.7 Hz), 6.86 (1H, *d*, *J* = 2.2 Hz), 6.95–6.97 (2H, *m*), 7.02 (1H, *d*, *J* = 2.0 Hz), 7.13–7.15 (3H, *m*), 7.24 (1H, *d*, *J* = 8,7 Hz), 9.04 (1H, *br. s*). $^{13}$C NMR (100 MHz, $CD_3CN$): δ 33.5, 37.6, 54.3, 103.6, 108.4, 112.8, 113.0, 125.9, 127.7, 129.3 (2), 130.2 (2), 132.3, 137.5, 151.5, 172.9 (2). MS (ESI): *m/z* 339 $[M+H]^+$. *6-OH-IAA-Phe (**14**)*. $^1$H NMR (400 MHz, $CD_3CN$): δ 2.92 (1H, *dd*, *J* = 7.6, 13.9 Hz), 3.06 (1H, *dd*, *J* = 5.2, 13.9 Hz), 3.54 (2H, *s*), 4.60 (1H, *dt*, *J* = 5.2, 7.6 Hz), 6.53 (1H, *d*, *J* = 6.8 Hz), 6.59 (1H, *dd*, *J* = 2.2, 8.5 Hz), 6.80 (1H, *d*, *J* = 2.0 Hz), 6.90 (1H, *d*, *J* = 2.3 Hz), 6.97–6.99 (2H, *m*), 7.15–7.18 (4H, *m*), 7.22 (1H, *d*, *J* = 8.6 Hz), 8.94 (1H, *br. s*). $^{13}$C NMR (100 MHz, $CD_3CN$): δ 33.5, 37.6, 54.2, 97.6, 109.2, 110.4, 120.2, 122.2, 123.6, 127.7, 129.3 (2), 130.2 (2), 137.6, 138.5, 154.1, 172.7, 172.9. MS (ESI): *m/z* 339 $[M+H]^+$. *7-OH-IAA-Phe (**30**)*. $^1$H NMR (400 MHz, $CD_3CN$): δ 2.92 (1H, *dd*, *J* = 7.6, 13.9 Hz), 3.05 (1H, *dd*, *J* = 5.1, 13.9 Hz), 3.60 (2H, *s*), 4.63 (1H, *dt*, *J* = 5.2, 7.7 Hz), 6.59 (1H, *d*, *J* = 7.5 Hz), 6.64 (1H, *d*, *J* = 7.6 Hz), 6.84 (1H, *dd*, *J* = 7.7, 7.8 Hz), 6.94–6.96 (3H, *m*), 7.00 (1H, *d*, *J* = 2.4 Hz), 7.13–7.15 (3H, *m*), 9.26 (1H, *br. s*). $^{13}$C NMR (100 MHz, $CD_3CN$): δ 33.5, 37.6, 54.4, 107.3, 109.5, 111.5, 121.0, 124.9,127.3, 127.7, 129.3 (2), 130.2 (2), 130.3, 137.5, 143.9, 173.2, 173.3. MS (ESI): *m/z* 339 $[M+H]^+$.

### 5.5. Deuterium-labeled compounds

[2′,2′-$^2H_2$]IAA-Asp (**2**-*d*$_2$) and [2′,2′-$^2H_2$]IAA-Glu (**3**-*d*$_2$) were kindly supplied by Dr. J. Hiratake (Institute for Chemical Research, Kyoto University). [2′,2′-$^2H_2$]6-OH-IAA-Val (**13**-*d*$_2$) and [2′,2′-$^2H_2$]6-OH-IAA-Phe (**14**-*d*$_2$) were deuterium-labeled according to the method of Hiratake et al. with some modification (Hiratake et al.,

unpublished data). [2′,2′-$^2H_2$]6-OH-IAA (**17**-$d_2$), [2′,2′-$^2H_2$]IAA-Glc (**9**-$d_2$), and [2′,2′-$^2H_2$]OxIAA-Glc (**10**-$d_2$) were synthesized by hydrogen/deuterium exchange reaction catalyzed by NaOD (manuscript in preparation). The isotopic purity of these compounds was checked by MRM-based LC–MS/MS analyses. Unlabeled (natural abundance) compound was not detected in each preparation, except for [2′,2′-$^2H_2$]6-OH-IAA (**17**-$d_2$); the purity of **17**-$d_2$ was 77.5%.

### 5.6. Root growth inhibition assay

Four-day-old seedlings grown vertically on 0.5 MS agar plates under continuous light were transferred to MS agar plates containing a given concentration of test compounds. The plates were kept vertically and incubated at 22 °C under continuous light for 5 days; lengths of primary root were recorded.

### 5.7. Administration experiments

Deuterium-labeled compounds (50 mM in EtOH) were diluted with distilled $H_2O$ to 100 μM. The solutions (1 ml) were individually applied to the surface of agar-solidified MS medium (30 ml) in which 2-week-old seedlings grew. After 48 h in the dark at 22 °C, samples for analysis were prepared by the procedure described above, but in this case purification by preparative HPLC was not performed. The incorporation of deuterium into metabolites was analyzed by LC-ESI-MS/MS.

### 5.8. Quantification of IAA (*1*) and its metabolites *2*, *3*, *6*, *9*, *10*, *13*, and *14*

Approximately 100–500 mg of plant tissue was homogenized in liquid $N_2$, and then in acetone–$H_2O$ (4:1, v/v) containing 2.5 mM diethyldithiocarbamic acid and a mixture of [$^{13}C_6$]-**1**, **2**-$d_2$, **3**-$d_2$, **6**-$d_2$, **9**-$d_2$, **10**-$d_2$, **13**-$d_2$, and **14**-$d_2$ (0.5 nmol each) were added as internal standards. The homogenate was then kept at 4 °C for 2 h. Following the separation of supernatant by decantation, the residue was again suspended with acetone–$H_2O$ (4:1, v/v) containing 2.5 mM diethyldithiocarbamic acid, and this procedure was repeated. The combined extracts were evaporated to remove acetone. After the pH was adjusted to approximately 2.6 with 2% (v/v) $HCO_2H$, the sample was subjected to solid-phase extraction as described above. After evaporation of the solvent, the sample was dissolved in $CH_3CN$–$H_2O$ containing 0.5% (v/v) AcOH (3:7, v/v).

IAA (**1**) and metabolites **2**, **3**, **6**, **9**, **10**, **13**, and **14** were quantified using the LC-ESI-MS/MS system as described above. The mobile phase was delivered at a flow rate of 200 μl/min with an initial mixture of MeOH–$H_2O$ containing 0.05% (v/v) AcOH (1:9, v/v) for 1 min, followed by a 14-min linear gradient to MeOH–$H_2O$ containing 0.05% (v/v) AcOH (9:1, v/v). The temperature was 30 °C. Other LC conditions were the same as those for the screening of metabolites. The mass spectrometer was operated in the MRM mode and its parameters are shown in Table 3.

## Acknowledgements

We thank Dr. Jun Hiratake of the Institute for Chemistry, Kyoto University, for the gift of the deuterium-labeled IAA-amino acids. This work was supported by CREST of the Japan Science and Technology Agency (JST).

## References

Bandurski, R., Cohen, J., Slovin, J., Reinecke, D., 1995. Auxin biosynthesis and metabolism. In: Davies, P. (Ed.), Plant Hormones: Physiology, Biochemistry and Molecular Biology. Kluwer Academic Publishers, Dordrecht, pp. 39–65.

Barratt, N.M., Dong, W., Gage, D.A., Magnus, V., Town, C.D., 1999. Metabolism of exogenous auxin by *Arabidopsis thaliana*: identification of the conjugate $N_\alpha$-(indol-3-ylacetyl)-glutamine and initiation of a mutant screen. Physiol. Plant. 105, 207–217.

Bartel, B., Fink, G.R., 1995. ILR1, an amidohydrolase that releases active indole-3-acetic acid from conjugates. Science 268, 1745–1748.

Bialek, K., Cohen, J.D., 1986. Isolation and partial characterization of the major amide-linked conjugate of indole-3-acetic acid from *Phaseolus vulgaris* L.. Plant Physiol. 80, 99–104.

Davies, R.T., Goetz, D.H., Lasswell, J., Anderson, M.N., Bartel, B., 1999. IAR3 encodes an auxin conjugate hydrolase from *Arabidopsis*. Plant Cell 11, 365–376.

Feung, C., Hamilton, R.H., Mumma, R.O., 1976. Metabolism of indole-3-acetic acid. Plant Physiol. 58, 666–669.

Jackson, R.G., Lim, E.K., Li, Y., Kowalczyk, M., Sandberg, G., Hoggett, J., Ashford, D.A., Bowlws, D.J., 2001. Identification and biochemical characterization of an *Arabidopsis* indole-3-acetic acid glucosyltransferase. J. Biol. Chem. 276, 4350–4356.

Jackson, R.G., Kowalczyk, M., Li, Y., Higgins, G., Ross, J., Sandberg, G., Bowles, D.J., 2002. Over-expression of an *Arabidopsis* gene encoding a glucosyltransferase of indole-3-acetic acid: phenotypic characterization of transgenic lines. Plant J. 32, 573–583.

Kowalczyk, M., Sandberg, G., 2001. Quantitative analysis of indole-3-acetic acid metabolites in *Arabidopsis*. Plant Physiol. 127, 1845–1853.

Kumer, S.C., Vrana, K.E., 1996. Intricate regulation of tyrosine hydroxylase activity and gene expression. J. Neurochem. 67, 443–462.

Lasswell, J., Rogg, L.E., Nelson, D.C., Rongey, C., Bartel, B., 2000. Cloning and characterizarion of *IAR1*, a gene requires for auxin conjugate sensitivity in *Arabidopsis*. Plant Cell 12, 2395–2408.

LeClere, S., Tellez, R., Rampey, R.A., Matsuda, S.P.T., Bartel, B., 2002. Characterization of a family of IAA-amino acid conjugate hydrolases from *Arabidopsis*. J. Biol. Chem. 277, 20446–20452.

Ljung, K., Hull, A.K., Kowalczyk, M., Marchant, A., Celenza, J., Cohen, J.D., Sandberg, G., 2002. Biosynthesis, conjugation, catabolism and homeostasis of indole-3-acetic acids in *Arabidopsis thaliana*. Plant Mol. Biol. 50, 309–332.

Normanly, J., 1997. Auxin metabolism. Physiol. Plant. 100, 422–431.

Normanly, J., Bartel, B., 1999. Redundancy as a way of life-IAA metabolism. Curr. Opin. Plant Biol. 2, 207–213.

Östin, A., Catalá, C., Chamarro, J., Sandberg, G., 1995. Identification of glucopyranosyl-β-1,4-glucopyranosyl-β-1-*N*-oxindole-3-acetyl-*N*-aspartic acid, a new IAA catabolite, by liquid chromatography/tandem mass spectrometry. J. Mass Spectrom. 30, 1007–1017.

Östin, A., Kowalyczk, M., Bhalerao, R.P., Sandberg, G., 1998. Metabolism of indole-3-acetic acid in *Arabidopsis*. Plant Physiol. 118, 285–296.

Park, S., Cohen, J.D., Slovin, J.P., 2006. Strawberry fruit protein with a novel indole-acyl modification. Planta 224, 1015–1022.

Rampey, R.A., LeClere, S., Kowalczyk, M., Sandberg, G., Bartel, B., 2004. A family of auxin-conjugate hydrolases that contributes to free indole-3-acetic acid levels during *Arabidopsis* germination. Plant Physiol. 135, 978–988.

Schmidt, R.R., Michel, J., 1985. *O*-(α-D-Glucopyranosyl)trichloroacetimidate as a glucosyl donor. J. Carbohydr. Chem. 4, 141–169.

Slovin, J.P., Bandurski, R.S., Cohen, J.D., 1999. Auxin. In: Hooykaas, P., Libbenga, K. (Eds.), Biochemistry and Molecular Biology of Plant Hormones. Elsevier Science, Oxford, pp. 115–140.

Staswick, P.E., Serban, B., Rowe, M., Tiryaki, I., Maldonado, M.T., Maldonado, M.C., Suza, W., 2005. Characterization of an *Arabidopsis* enzyme family that conjugates amino acids to indole-3-acetic acid. Plant Cell 17, 616–627.

Szerszen, J.B., Szczyglowski, K., Bandurski, R.S., 1994. *iaglu*: a gene from *Zea mays* involved in conjugation of growth hormone indole-3-acetic acid. Science 265, 1699–1701.

Tam, Y.Y., Epstein, E., Normanly, J., 2000. Characterization of auxin conjugates in *Arabidopsis*. Low steady-state levels of indole-3-acetyl-aspartate, indole-3-acetyl-glutamate, and indole-3-acetyl-glucose. Plant Physiol. 123, 589–595.

Tuominen, H., Östin, A., Sandberg, G., Sundberg, B., 1994. A novel metabolic pathway for indole-3-acetic acid in apical shoot of *Populus tremula* (L.) × *Populus tremuloides* (Michx.). Plant Physiol. 106, 1511–1520.

Walz, A., Park, S., Slovin, J.P., Ludwig-Müller, L., Momonoki, Y.S., Cohen, J.D., 2002. A gene encoding a protein modified by the phytohormone indoleacetic acid. Proc. Natl. Acad. Sci. USA 99, 1718–1723.

Woodward, A.W., Bartel, B., 2005. Auxin: regulation, action, and interaction. Ann. Bot. 95, 707–735.